Journal of Hydrology 381 (2010) 203–212

Contents lists available at ScienceDirect

Journal of Hydrology

journal homepage: www.elsevier.com/locate/jhydrol

A regional snow-line method for estimating snow cover from MODIS during cloud cover

J. Parajka [a,b,*], M. Pepe [c], A. Rampini [c], S. Rossi [d], G. Blöschl [a]

[a] Institute for Hydraulic and Water Resources Engineering, Vienna University of Technology, Austria
[b] Institute of Hydrology, Slovak Academy of Sciences, Liptovsky Mikulas, Slovakia
[c] Consiglio Nazionale delle Ricerche, IREA, Via Bassini 15, 20133 Milano, Italy
[d] European Commission Joint Research Centre, Institute for Environment and Sustainability, Ispra (VA), Italy

ARTICLE INFO

Article history:
Received 22 April 2009
Received in revised form 23 November 2009
Accepted 25 November 2009

This manuscript was handled by K. Georgakakos, Editor-in-Chief

Keywords:
MODIS
Snow cover
Mapping
Clouds

SUMMARY

The objective of this study is to propose and evaluate a method for snow cover mapping during clouds using the daily MODIS/Terra snow cover product. The proposed *SNOWL* approach is based on reclassifying pixels assigned as clouds to snow or land according to their relative position to the regional snow-line elevation. The accuracy of the *SNOWL* approach is evaluated over Austria, using daily snow depth measurements at 754 climate stations and daily MODIS/Terra images in the period July 2002–December 2005. The results indicate that the *SNOWL* method provides a robust snow cover mapping over the entire region even if the MODIS/Terra cloud cover is as large as 90%. Cloudiness is decreased from 60% (MODIS/Terra) to 10% (*SNOWL*) without hardly any change in mapping accuracy. Sensitivity analyses indicate that the estimation of the regional snow-line elevation is particularly sensitive to the misclassification of cirrus clouds as snow in the period between May and October.

Introduction

Seasonal accumulation of precipitation in the form of snow and its release through snowmelt runoff is an important component of the hydrologic cycle in many regions of the world. Snow cover mapping is particularly important in mountains where, often, an increased demand for water resources leads to a conflict between human needs and the needs to sustain freshwater ecosystems. Since the mid-1970s a variety of remote sensing products has been used to map the changes in snow cover from global to catchment scales. In recent years, numerous applications of daily MODerate-resolution Imaging Spectroradiometer (MODIS) snow cover products have demonstrated their high accuracy and consistency with ground based snow observations (see e.g., Klein and Barnett, 2003; Maurer et al., 2003; Simic et al., 2004; Zhou et al., 2005; Pu et al., 2007; Wang et al., 2008). As summarized by Hall and Riggs (2007), the overall absolute accuracy of daily MODIS images is about 93%, but this corresponds only to clear sky conditions. In many regions, the persistent cloud coverage can significantly limit MODIS application for snow cover mapping and its usefulness for assimilation into hydrologic models. As shown in Parajka and Blöschl (2006), for example, clouds cover 63% of Austria on average and cloud coverage is even larger in the winter. A similar average cloud cover of about 70% is indicated by Tong et al. (2009) for the Quesnel River Basin (British Columbia, Canada) and 50–60% by Gao et al. (submitted for publication) for Alaska. However, as indicated by several studies, cloud reduction in the images is possible. The approaches used for cloud reclassification are based either on the use of information from neighbouring non-cloud covered pixels in time or space (temporal and spatial filters) or the combination with products from different platforms. Parajka and Blöschl (2008) combined images from two MODIS platforms (Terra and Aqua) and evaluated various temporal and spatial filters over Austria. They reported a reduction of clouds from 63% to 55% and 4% by combining Terra and Aqua and a 7-day temporal filter, respectively. Gao et al. (submitted for publication) combined Terra and Aqua over Alaska and found a reduction in cloud coverage of 12% against Aqua and 7% against Terra products. Wang et al. (2008) and Xie et al. (2009) obtained a 10% cloud reduction for the northern Xinjiang (China) region. An approach that combines MODIS images with the passive microwave AMSR-E product is presented by Liang et al. (2008). They investigated the pros and cons of passive microwave imagery, which is their availability in all weather conditions, but their coarse spatial resolution (25 km for the AMSR-E compared to 500 m of MODIS). They found that the

* Corresponding author. Address: Institute for Hydraulic and Water Resources Engineering, Vienna University of Technology, Karlsplatz 13/222, A-1040 Vienna, Austria. Tel.: +43 1 58 801 223 01; fax: +43 1 58 801 223 99.
E-mail address: parajka@hydro.tuwien.ac.at (J. Parajka).

0022-1694/$ - see front matter
doi:10.1016/j.jhydrol.2009.11.042

agreement of the combined MODIS–AMSR-E product with the in situ measurements at 20 stations was 75%, instead of 34% for the MODIS daily product in all weather conditions. Recently, Gao et al. (submitted for publication) replaced the MODIS cloud pixels by AMSR-E pixels. Such a combination resulted in a further increase in the accuracy related to all weather conditions.

Other approaches on higher resolution imagery, such as LANDSAT MSS and TM, are based on the recognition in the same image of cloud-free pixels with comparable snow conditions of cloud-obscured ones (Seidel et al., 1983, 1996; Pepe et al., 2005). Such similarity conditions are usually determined with the aid of ancillary data accounting for landscape conditions of the ground surface such as relief information (elevation, slope, aspect) and/or thematic entities (basin boundaries, elevation zones, land cover type). Pepe et al. (2005) demonstrated that this similarity approach works well in the Northern Italy. However it involves the assumption of meteorological homogeneity which is not always valid. It would be interesting to adopt this idea to cloud removal of MODIS images.

The objective of this paper is to propose and test this type of method for cloud reduction in the daily MODIS snow cover dataset. The basic idea of this approach is to estimate the regional snowline elevation and to reclassify the pixels assigned as clouds to snow or land categories according to their vertical position relative to the regional snow-line. The method, termed *SNOWL*, is based on similarity conditions but the introduction of a soft approach in transition areas allows to compensate the heterogeneity of meteorological conditions at a regional scale, avoiding the use of complex modeling. The accuracy of the *SNOWL* results is tested against in situ snow depth observations, and the effect of cloud cover on the robustness of the method is investigated.

The paper is organized as follows. First, the *SNOWL* mapping method is introduced and the methodology used for the validation is presented. Next, the study region and the MODIS and snow depth data used are described. The results show the potential and accuracy of proposed methodology, which are further discussed in the context of existing mapping approaches in the discussion and conclusions section.

Methods

Regional snowline mapping approach (SNOWL)

The cornerstone of the regional snowline mapping approach (*SNOWL*) is a reclassification of pixels assigned as clouds based on the assessment of the topographical elevation of pixels classified as snow and no snow (land). Specifically, the elevation of each pixel classified as clouds is compared with the mean elevation of all snow (μ_S) and land (μ_L) pixels, respectively. In the case the elevation of the cloud covered pixel is above the μ_S of the regional snow-line the pixel is assigned as snow covered. If the elevation is below the μ_L of the regional "land-line", the pixel is assigned as land. In the case the elevation is in between μ_S and μ_L, the pixel is assigned as partially snow covered. However, this procedure may not work well if the cloud coverage of the entire domain is large, i.e., there are only a few pixels from which the μ_S of the regional snow-line and the μ_L of the regional land-line can be extracted. A cloud cover threshold ζ_C was hence assumed. If the cloud coverage of the entire domain for a given day is smaller or equals ζ_C the procedure was performed as summarized above. If the cloud coverage was larger than ζ_C, the original classes (snow, land, clouds) were retained for this day.

Sensitivity analysis of SNOWL

In order to ensure the robustness of the *SNOWL* approach, a sensitivity analysis was performed. The main goal was to optimise the *SNOWL* method to minimise the cloud coverage and maximise the mapping accuracy. The sensitivity evaluation covers three main aspects: (a) the assessment of the frequency of MODIS snow cover images with cloud coverage larger than a predefined threshold ζ_C; (b) the assessment of the effect of the amount of cloud coverage on the estimation of the μ_S and μ_L; and (c) the testing of options for minimising the influence of misclassification of cirrus clouds as snow in the summer period.

The relative frequency of MODIS/Terra products over Austria (2002–2005), with cloud coverage larger than different thresholds ζ_C is summarized in Table 1. This evaluation shows that, overall, 57% of the available images have a cloud coverage larger than 60%, and 15% of the images have a cloud coverage larger than 95% of the territory of Austria. Clear days are not frequent, less than 9% of days have a cloud coverage less than 10%. Seasonally, clouds are somewhat more frequent in the winter than in the summer. For example, November, December and January have, on average, only 2–4% of days with less than 10% clouds, but in May, June and July the number of days with low cloud coverage increases to 10–12%.

The cloud cover extent affects not only the availability of snow cover information, but also has an impact on estimation of the regional snow- (μ_S) and land- (μ_L) lines. In order to evaluate the effects of clouds on μ_S and μ_L, two comparisons were plotted in Fig. 1. The top panels show the seasonal variability in the mean monthly elevation $\bar{\mu}_S$ and $\bar{\mu}_L$ for different cloud thresholds ζ_C. The bottom panels show the within-month variability of the regional snow- and land-line elevations expressed by the standard deviation of μ_S and μ_L within a particular month. It is clear that the seasonal variation of both, the mean and the standard deviation

Table 1
Frequency (%) of MODIS/Terra snow cover images with cloud coverage larger than different thresholds ζ_C for Austria.

Season	ζ_C = 10%	ζ_C = 60%	ζ_C = 80%	ζ_C = 90%	ζ_C = 95%	ζ_C = 98%	ζ_C = 99%
January	95.7	74.2	51.6	30.1	19.4	8.6	6.5
February	91.6	61.4	39.8	20.5	16.9	8.4	4.8
March	89.2	53.8	35.5	21.5	14.0	5.4	5.4
April	94.4	60.0	37.8	27.8	17.8	8.9	6.7
May	88.2	63.4	35.5	22.6	17.2	9.7	5.4
June	90.0	55.6	30.0	16.7	7.8	4.4	2.2
July	88.7	51.6	33.9	20.2	11.3	6.5	3.2
August	93.5	43.5	25.8	16.1	15.3	9.7	7.3
September	78.3	46.7	31.7	20.0	13.3	9.2	5.0
October	94.4	49.2	31.5	20.2	12.1	6.5	4.8
November	98.3	75.0	52.5	30.0	19.2	11.7	8.3
December	97.3	60.7	40.2	30.4	19.6	11.6	7.1
Annual mean	91.6	57.3	36.9	22.9	15.2	8.5	5.6

July 2002–December 2005 (1266 available images).

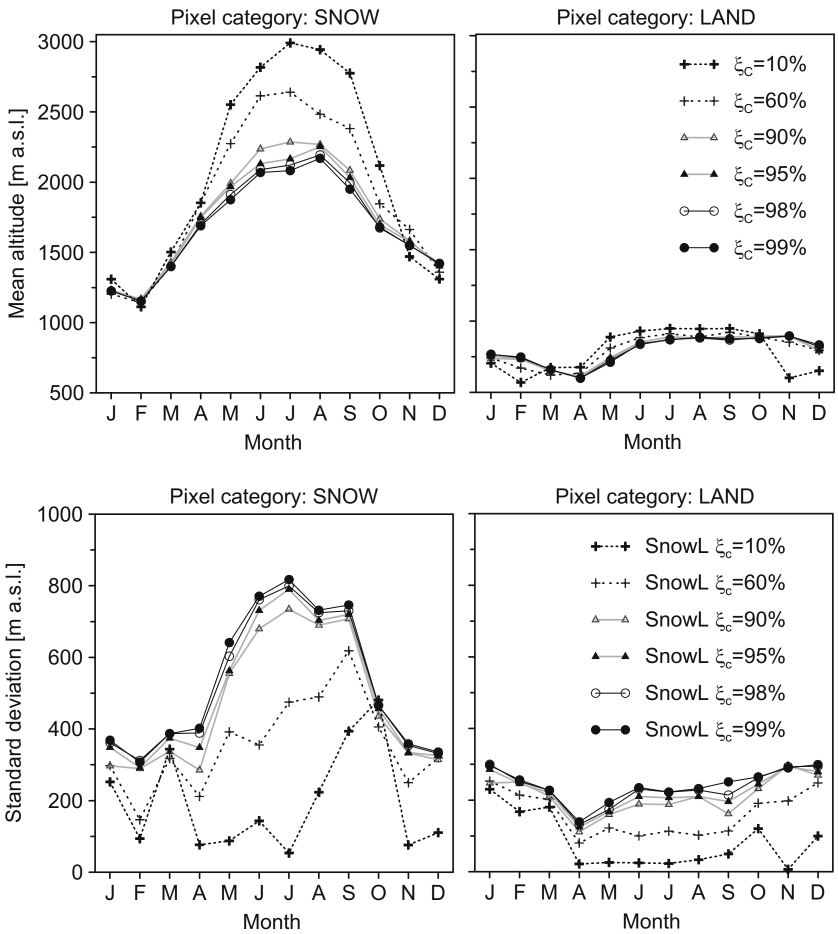

Fig. 1. Elevation of mean monthly regional snow- and land-lines (top) and their within-month variability (bottom) evaluated seasonally for different cloud thresholds ζ_C in the period July 2002–December 2005. The threshold e.g., $\zeta_C = 60\%$ means that the mean regional snow- or land-line elevation were calculated only for days with cloud coverage less than 60%.

of μ_S and μ_L, is generally higher than the differences due to the ζ_C. An exception are the results for $\zeta_C = 10\%$, which are, however, based on only a small number (less than 9%, Table 1) of MODIS images. The figure shows that the mean land-line elevation $\bar{\mu}_L$ varies between 650–700 m a.s.l. and 850–900 m a.s.l. in the cold and warm seasons, respectively. The mean snow-line elevation $\bar{\mu}_S$ varies between 1200 and 1250 m a.s.l. in January and February and around 2000 m a.s.l. in June, July and August. The evaluation of the within-month variability of the regional snow- and land-lines (Fig. 1 bottom) indicates that the mean elevation of snow or land pixels varies significantly from day to day. Generally, the standard deviations of μ_S are higher than those of μ_L and both increase with increasing cloud threshold ζ_C. The largest seasonal differences are observed for the standard deviations of μ_S, where a significant increase in the variability occurs in the period between May and October. This increase is caused, on the one hand, by a natural increase in the occurrence of short snow periods especially in the mountains. On the other hand, it is partly due to the misclassification of cirrus clouds as snow. As documented, e.g., in Riggs et al. (2003), the liberal cloud mask used in the original MODIS/Terra mapping approach (version V004) is prone to incorrectly labeling ice clouds as snow. Parajka and Blöschl (2006) indicated that, in Austria, almost all MODIS overestimation errors in the summer months were caused by the misclassification of cirrus clouds as snow. In order to investigate the frequency of such cases, a comparison with grid maps of mean daily air temperatures was performed. Table 2 summarizes the number of pixels classified as snow when the mean daily air temperature was above 10 °C related to the total number of pixels in Austria (in %). The mean represents the daily average in a particular month, the percentile shows the frequency in which 90% of pixels are below this value and maximum shows the maximum spatial coverage of this type of misclassification observed in different seasons in the period between July 2002 and December 2005. Interestingly, Table 2 also shows the mean daily difference in μ_S, calculated from all pixels classified as snow minus the elevation of snow pixels with air temperature below 10 C. It is clear that the misclassification is observed only on a small part of the region, but may have a significant influence on the calculation of μ_S in the period between May and October.

The results of the sensitivity analyses suggest that the robustness of the general *SNOWL* mapping approach will be enhanced by using the following settings:

(a) the reclassification of clouds is performed for days where at least 1% of Austria is classified either as land or snow,
(b) the estimation of the regional snow- and land-lines is based on daily basis,
(c) pixels classified as snow are reclassified to land in the cases that they cover less than 1% of Austria in the period between May and October and are located at elevations above 3000 m a.s.l.

These settings were applied for snow cover mapping and the accuracy assessment in the remainder of this paper. In order to shed more light on the effects of different cloud thresholds ζ_C, this

Table 2
Frequency of pixels (in % of Austria) classified as snow when the mean daily air temperature was above 10 °C.

Season	Mean	P90%	Max.	Elevation difference (m a.s.l.)
January	0.0	0.0	0.0	0
February	0.0	0.0	0.9	0
March	0.0	0.1	2.7	−6
April	0.0	0.3	1.1	−38
May	0.1	0.8	3.2	−216
June	0.1	0.4	1.9	−433
July	0.0	0.3	1.4	−448
August	0.1	0.3	1.5	−555
September	0.1	0.4	1.7	−392
October	0.0	0.6	1.9	−154
November	0.0	0.1	1.2	−8
December	0.0	0.0	0.0	0

Seasonal mean, percentile P90% and maximum frequencies calculated from daily MODIS/Terra images in the period from July 2002 to December 2005 (1266 images). The mean daily elevation difference expresses the disagreement between the regional snow-line elevation (μ_S) estimated from all snow covered pixels minus regional snow-line elevation of pixels with air temperature below 10 °C.

threshold was not fixed and different ζ_C values were applied in the evaluations.

SNOWL accuracy assessment

The accuracy of the *SNOWL* mapping approach was quantitatively evaluated using ground snow depth measurements. Snow depth observations at the climate stations were considered as ground truth for the pixel that was closest to each station. The overall degree of agreement between the *SNOWL* images and snow depth measurements was represented by the accuracy indices k_C and k_{CF}. These are defined as the sum of correctly classified station-days divided by the total number of station-days (k_C) and cloud-free station-days (k_{CF}) in %, respectively. The correctly classified station-days include the following cases:

(a) snow at the *SNOWL* pixel and snow (1 cm and above) at the climate station,
(b) no snow at the *SNOWL* pixel and no snow (0 cm) at the climate station,
(c) partial snow cover at the *SNOWL* pixel and snow depth in the range 0–3 cm at the climate station.

A more detailed evaluation and discussion about the threshold definition is presented in Parajka and Blöschl (2008). The station-days are defined here as the number of days of misclassification or correct classification summed over all stations and evaluated either for individual months or for the entire period from July 2002 to December 2005. The misclassification of snow as land was additionally evaluated as the *SNOWL* underestimation error (*SU*) and the misclassification of land as snow was evaluated as the *SNOWL* overestimation error (*SO*). Both relate the sum of misclassified station-days to the total number of cloud-free station-days (in %).

Data

Study area

The *SNOWL* mapping approach was tested over Austria. This region covers an area of about 84,000 km^2 and is characterized by mountain terrain in the West and South and flat or undulating topography in the East and North (Fig. 2). Elevations range from 115 m a.s.l. to 3797 m a.s.l. Land use is mainly agricultural in the lowlands and forest in the medium elevation ranges. Alpine vegetation and rocks prevail in the highest mountain regions. Climatologically, Austria is situated in the temperate zone at the border between the Atlantic and the continental part of Europe. Mean annual temperature varies from about 10 °C in the lowlands to less than −8 °C in the Alps. The mean annual precipitation varies from less than 400 mm/year in the East to almost 3000 mm/year in the West. Such diverse climatic, physiographic and landscape characteristics probe Austria an ideal testbed for the method, so the results of the snow cover mapping should be applicable to a wider domain with similar characteristics.

MODIS

The MODIS/Terra Snow Cover Daily L3 Global 500 m Grid (MOD10A1) dataset was used. MODIS is an optical instrument mounted on the Terra satellite of the NASA Earth Observation

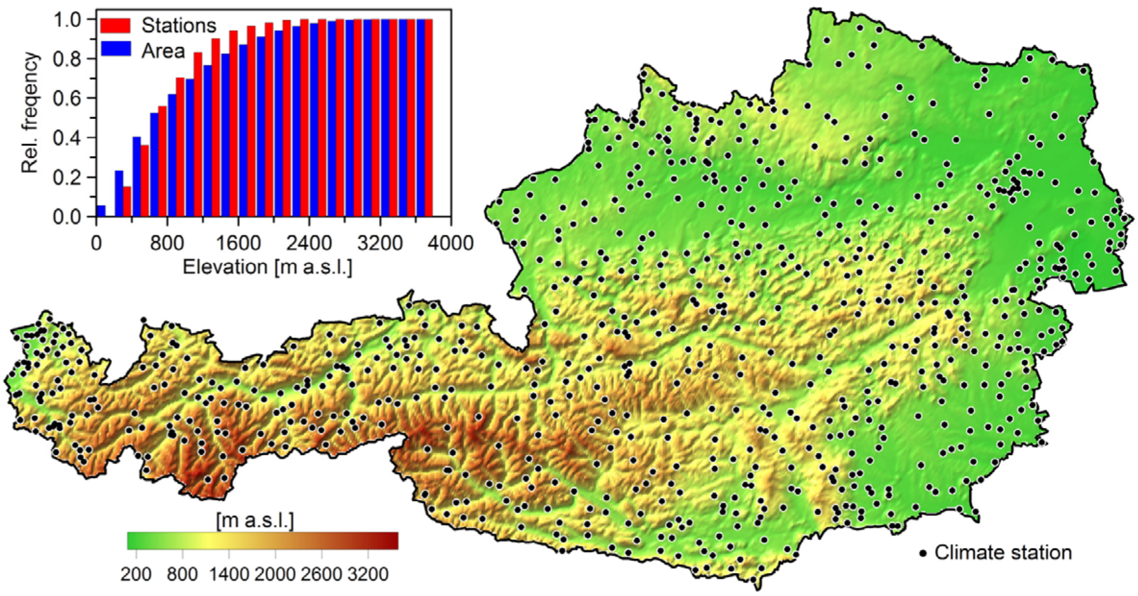

Fig. 2. Study area and location of climate stations. The histograms show the relative cumulative frequency of the climate stations (red bars) and the area (blue bars) for different elevation zones. (For interpretation of the references to colour in this figure legend, the reader is referred to the web version of this article.)

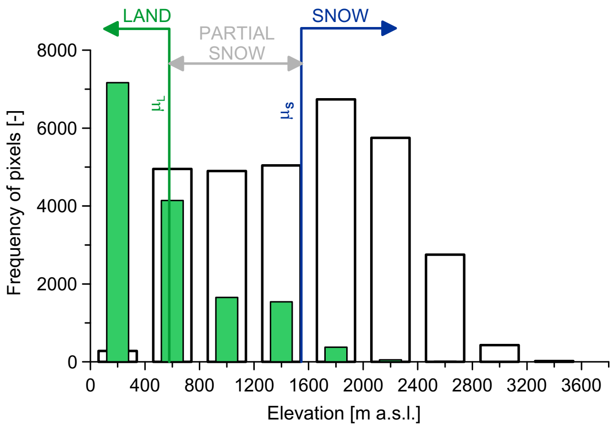

Fig. 3. Elevation distribution of pixels classified as snow (white bars) and land (green bars) on January 23, 2003. The mean elevation of pixels classified as snow μ_S is 1550 m a.s.l., that for land μ_L is 590 m a.s.l. (For interpretation of the references to colour in this figure legend, the reader is referred to the web version of this article.)

System. The basic principle of the snow cover mapping is based on the difference between the infrared reflectance of snow in visible and short-wave wavelengths, threshold-based criteria tests, and decision rules. Details of the mapping algorithm are given in the Algorithm Theoretical Basis Document (Hall et al., 2001) and on the NSIDC web page (www.nsidc.org).

In this study version 4 (V004) was applied using daily snow cover images in the period July 2002–December 2005. Austria is covered by the h18v04 and h19v04 tiles with 500 m spatial resolution. We combined data from both tiles and reprojected them to Lambert conformal conic projection using MODIS Reprojection Tool (MRT, 2004). After the transformation, we reclassified the MODIS snow cover maps from originally 16 pixel classes to three classes: snow, land and clouds (including missing and erroneous data). These snow cover maps were subsequently used for testing the *SNOWL* algorithm.

Snow depth observations

For the quantitative validation of the *SNOWL* mapping approach, the snow depth observations at 754 climate stations were used. This dataset includes the snow depth readings performed daily at 7:00 AM in the period from July 2002 to December 2005. The locations of these point measurements are shown in Fig. 2. The snow depth measurements cover a wide range of elevation zones, but, in the mountain regions, the stations tend to be located at lower elevations, typically in the valleys. The highest climate station is situated at 2290 m a.s.l. which means that 6% of Austria (area above that elevation) is not represented by any climate station.

Results

An example of the application of *SNOWL* is presented in Figs. 3 and 4. Fig. 3 shows the distribution of different elevation classes for pixels classified as snow and land on January 23, 2003. From this distribution, the elevation of the regional snow- and land-lines were estimated as 1550 m a.s.l. (μ_S) and 590 m a.s.l. (μ_L), respectively. This means that in *SNOWL* cloud pixels below 590 m a.s.l. are reclassified as land, cloud pixels above 1550 m a.s.l. are reclassified as snow, and cloud pixels in between these elevation thresholds are reclassified as partially snow covered. The spatial result of this reclassification procedure is presented in Fig. 4. The top panel shows the original MODIS/Terra image, the middle panel presents the result of the *SNOWL* algorithm and the bottom panel shows the snow depth observations at the climate stations. The comparison of spatial patterns indicates generally very good agreement with the snow depth observations, even though clouds cover 85% of Austria.

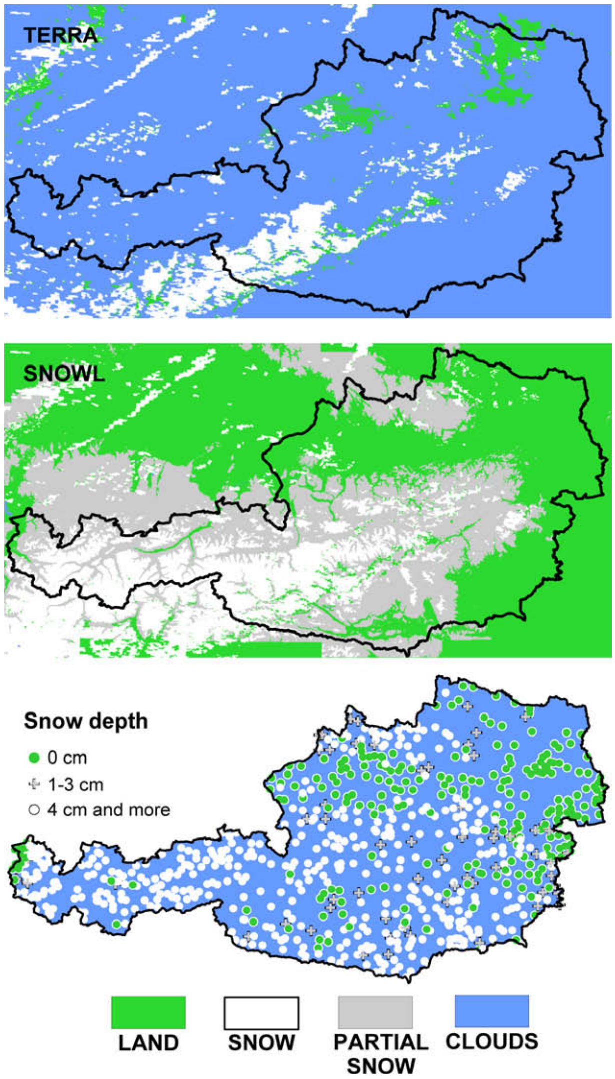

Fig. 4. Example of the *SNOWL* mapping approach on January 23, 2003. The top panel shows the original MODIS/Terra image, the middle panel a replacement of cloud pixels by the *SNOWL* mapping approach, and the bottom panel the snow depth observations at the climate stations. Cloud coverage is approximately 85%.

The seasonal evaluation of the cloud, snow, partial snow cover and the snow covered area (SCA) characteristics is presented in Fig. 5. The cloud (and similarly snow and partial snow) coverage is defined as the number of cloud (snow and partial snow) pixels divided by the total number of pixels over Austria in particular month. The SCA is defined as the number of snow pixels divided by the number of snow and land pixels. The assessment compares the original MODIS/Terra dataset (diamonds) with the *SNOWL* approach based on different cloud threshold ζ_C. The results show the efficiency of the *SNOWL* to reduce clouds. The monthly cloud coverage decreases from more than 60% (original MODIS/Terra) to less than 20% ($\zeta_C = 99\%$) in the winter and spring months. An exception is April, when the frequency of persistent cloud coverage is the largest. In the winter period (December–March), the snow coverage increases from 15–30% (MODIS/Terra) to 25–40% (*SNOWL* with $\zeta_C = 90\%$) and to 30–50% (*SNOWL* with $\zeta_C = 99\%$), respectively.

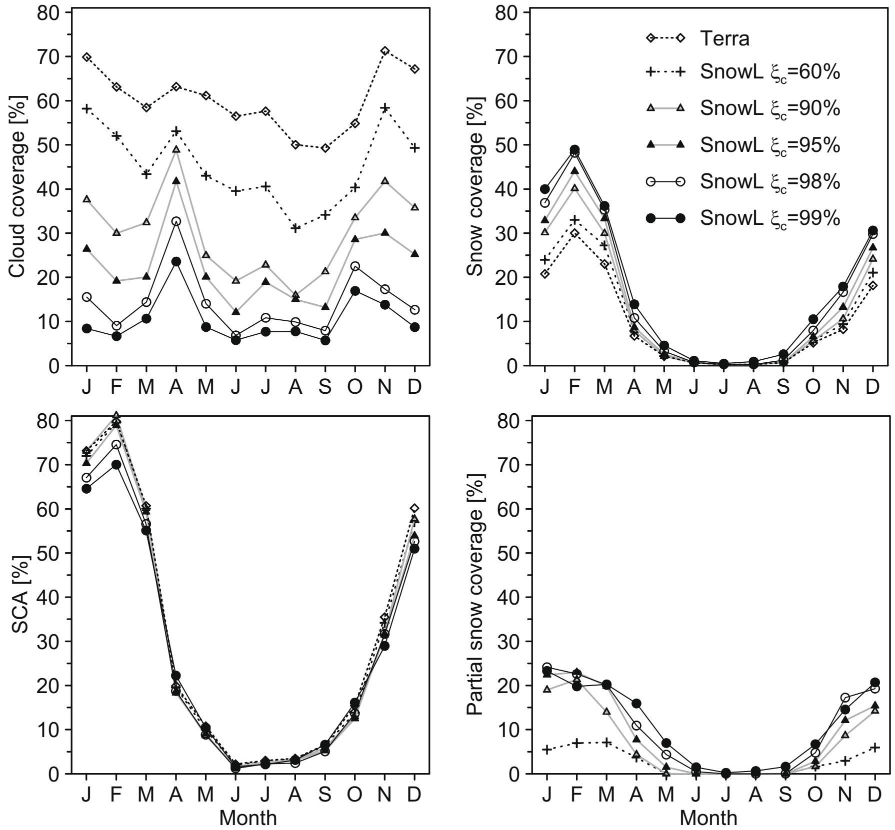

Fig. 5. Mean seasonal cloud, snow and partial snow cover and SCA estimated from the original MODIS/Terra and the *SNOWL* images in the period July 2002–December 2005. For the *SNOWL* method, different cloud thresholds (ζ_C) were applied.

Interestingly, the comparison of SCA coverage indicates very similar temporal patterns for both the original MODIS/Terra and *SNOWL* images. The differences between the SCA are small, only for February the difference between the MODIS/Terra and *SNOWL* (ζ_C = 99%) are larger than 10%. The evaluation of the *SNOWL* partial snow cover extent indicates that this category covers less than 10% and around 20–25% of Austria for the thresholds ζ_C = 60% and ζ_C = 90%, respectively.

The overall accuracy assessment of the original MODIS/Terra and *SNOWL* snow cover maps is presented in Fig. 6. The left panel compares the seasonal variability in the accuracy index k_{CF}, which is based on the evaluation of cloud-free stations days. The right panel shows the seasonal variability of the k_C index, which considers clouds as a false classification. The comparison indicates that the overall accuracy k_{CF} is practically the same for the original MODIS/Terra and *SNOWL* datasets with thresholds ζ_C = 90% and

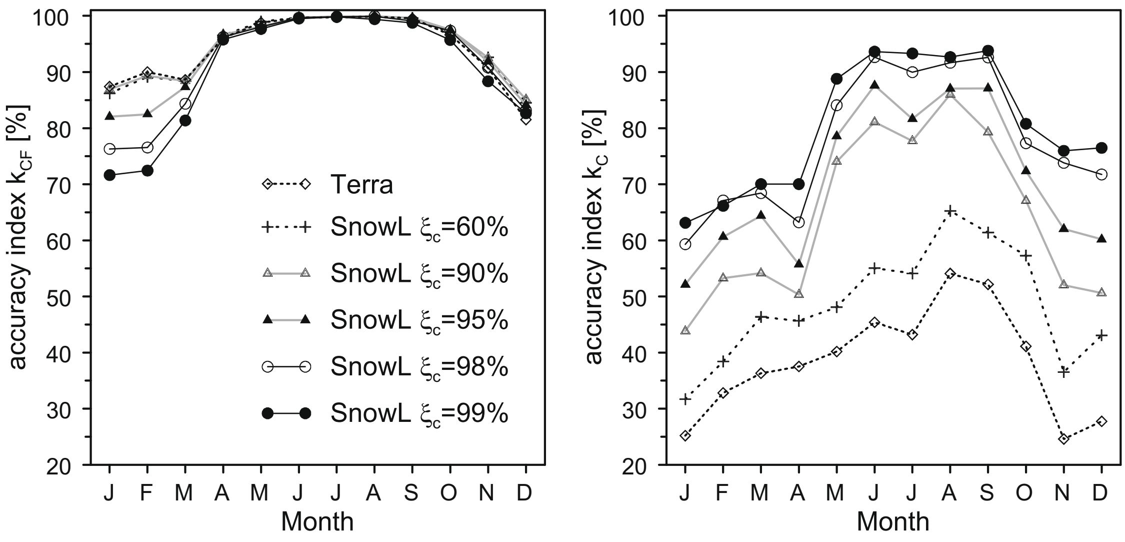

Fig. 6. Seasonal variability in the k_{CF} (cloud-free) and k_C (all days) and accuracy indices.

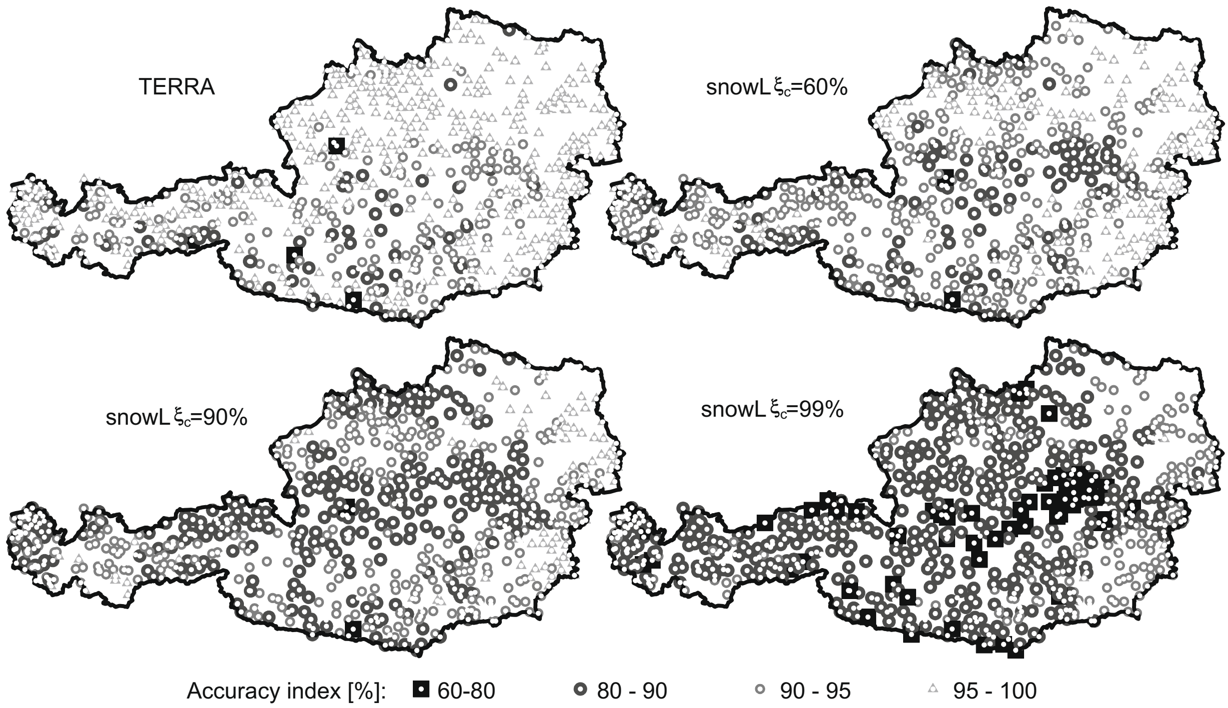

Fig. 7. Spatial variability in the k_{CF} accuracy index evaluated for different cloud thresholds ζ_C. The accuracy index k_{CF} is evaluated for cloud-free pixels in the period July 2002–December 2005.

lower. However, the k_{CF} accuracy decreases for ζ_C larger than 95% in the period between January and April. This decrease is around 5% and 15% for ζ_C = 95% and ζ_C = 99%, respectively. Much larger differences are observed for the k_C accuracy assessment. The *SNOWL* images have significantly higher k_C accuracy than the MODIS/Terra dataset under all weather conditions. The results indicate that, not surprisingly, k_C increases with increasing cloud thresholds ζ_C. In the period between November and March, k_C is about 20% higher for the *SNOWL* (ζ_C = 90%) than the original MODIS/Terra images. An even larger increase in the k_C accuracy is observed for ζ_C = 99%.

Fig. 7 gives the spatial accuracy patterns of the MODIS/Terra and *SNOWL* images for cloud-free days. It is clear that substitution of cloud pixels by the *SNOWL* approach increases the number of cloud-free pixels (depending on the ζ_C threshold), but decreases

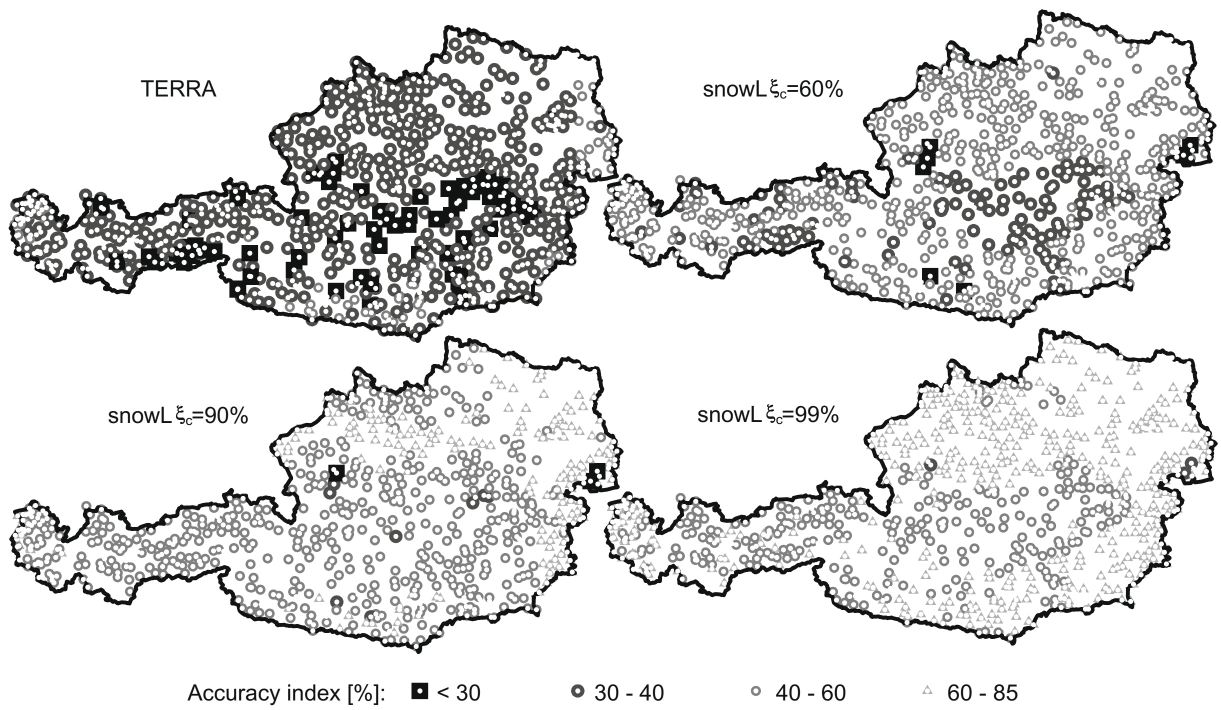

Fig. 8. Spatial variability in the k_C accuracy index evaluated for different cloud thresholds ζ_C. The accuracy index k_C is evaluated for all days in the period July 2002–December 2005.

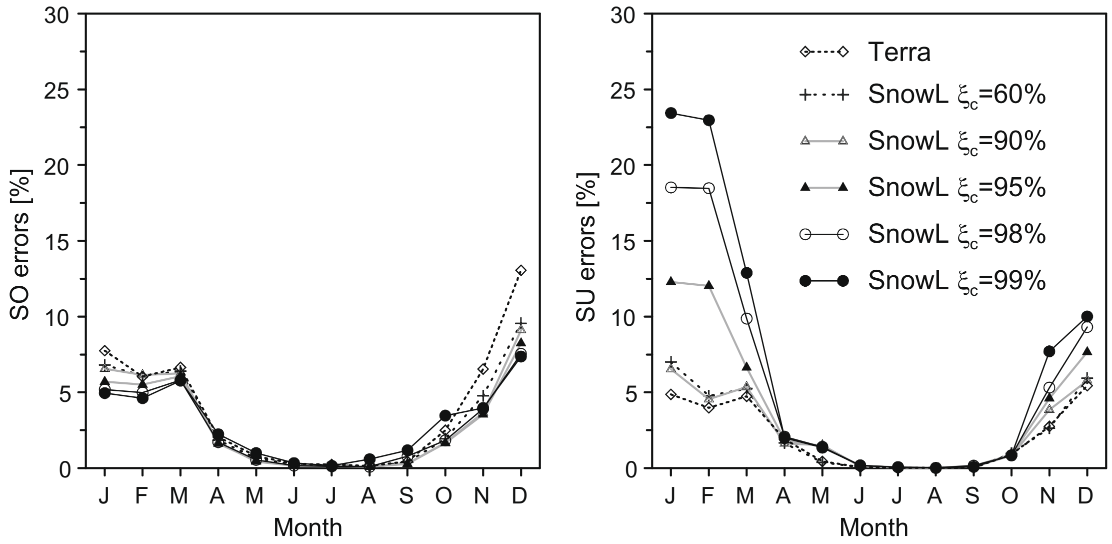

Fig. 9. Seasonal variability in the snow over- (*SO*) and under-estimation (*SU*) errors in the period July 2002–December 2005.

the k_{CF} accuracy measure. The number of stations with accuracy above 95% decreases from 467 stations for MODIS/Terra to 98 and 5 stations for *SNOWL* with $\zeta_C = 90\%$ and $\zeta_C = 99\%$, respectively. At the same time, the number of stations with the k_{CF} below 80% increases from 4 stations (MODIS/Terra) to 17 (*SNOWL* with $\zeta_C = 90\%$) and 61 stations (*SNOWL* with $\zeta_C = 99\%$). The spatial locations of the stations with poorer agreement indicate that they tend to group into a zone between 500 m a.s.l and 1500 m a.s.l., which corresponds to the transition zone between typical regional snow- and land-lines (Fig. 1). The spatial variability of the k_C index is given in Fig. 8. Generally, an increase in the cloud threshold ζ_C in the *SNOWL* maps leads to a remarkable increase in the overall accuracy k_C. The k_C values lower than 30% are observed at 78 stations for MODIS/Terra, but only at 7 stations for the *SNOWL* ($\zeta_C = 60\%$) method. The *SNOWL* maps based on $\zeta_C = 98\%$ and larger thresholds have no stations with k_C below 30% and only 4 stations with k_C below 40%. There is a remarkable increase in the number of stations with k_C above 60%, when the threshold ζ_C increases above 90%. These stations are located mainly in the flat and hilly regions of Austria. On the other hand, the stations with the largest k_C errors are mostly located in Alpine regions with most persistent cloud coverage (see e.g., Parajka and Blöschl (2006, 2008), where cloud cover evaluation over Austria was presented).

A more detailed evaluation of the error type, the over- (*SO*) and under- (*SU*) estimation errors, is presented in Fig. 9. The distribution of *SO* and *SU* errors corresponds to typical seasonal patterns of snow cover distribution, being larger in winter and very small in summer. The *SNOWL SO* errors are similar for different ζ_C and are generally somewhat smaller than obtained by MODIS/Terra. The largest *SO* errors, 7–9% for the *SNOWL* and 13% for Terra, are observed in December. The *SU* errors are of similar magnitude to the *SO* errors for $\zeta_C = 90\%$ and lower, but significantly larger for the *SNOWL* maps based on threshold $\zeta_C = 95\%$ and larger. This indicates that large cloud coverage (95% or more) does not enable a reliable estimation of the regional snow-line which tends to result in an underestimation of the snow cover.

Discussion and conclusions

This study proposes a method, *SNOWL*, for cloud reduction in MODIS snow cover images, which is based on the similarity in the vertical snow cover distribution over a region. This similarity is a key factor determining the applicability of such type of mapping method over wider spatial domains. We have evaluated this approach over Austria, which is an ideal testbed, because of its diverse climatic, physiographic and landscape characteristics. The accuracy assessment and sensitivity analyses showed that the *SNOWL* mapping method is remarkably robust including for cases where only a few percent of the pixels are cloud free. Estimation of the regional snow-line elevation is particularly sensitive to the misclassification of cirrus clouds as snow in the period between May and October. This misclassification occurs frequently, but tends to affect only a small area. This type of error significantly underestimates the snow-line elevation, which translates into poor mapping performance. In order to minimise this effect, we have applied a reclassification procedure, which replaces all snow pixels to land if they cover less than 1% of Austria in the period between May and October.

The assessment of the overall accuracy for cloud-free pixels indicates that the mapping performance of the *SNOWL* method is similar to the original MODIS/Terra and only somewhat decreases if clouds cover more than 90% of Austria. When considering clouds as false classification, the decrease in cloud extent by the *SNOWL* approach translates into a significantly higher mapping performance. The overall annual accuracy ranges from 48.7% to 81.5% depending on the cloud threshold used, compared to 38.5% for the original MODIS/Terra product. This difference in the mapping accuracy is similar to that obtained by Liang et al. (2008) who combined the daily MODIS/Terra data with the passive microwave imagery. They reported an overall accuracy of 75% for the

Table 3
Tradeoff between annual accuracy k_{CF} and cloud coverage for the original MODIS/Terra, the MODIS/Terra–Aqua combination, the 1- and 3-day filter applied on the combined Terra–Aqua (details are in Parajka and Blöschl (2008)) and different *SNOWL* mapping approaches.

Dataset	Accuracy k_{CF} (%)	Cloud coverage (%)
MODIS/Terra	95.1	60.1
Combined Terra + Aqua	94.9	55.3
Combined + 1-day filter	94.4	33.5
Combined + 3-day filter	93.3	15.5
SNOWL $\zeta_C = 60\%$	95.2	45.1
SNOWL $\zeta_C = 90\%$	95.8	30.2
SNOWL $\zeta_C = 98\%$	93.1	14.5
SNOWL $\zeta_C = 99\%$	91.5	10.4

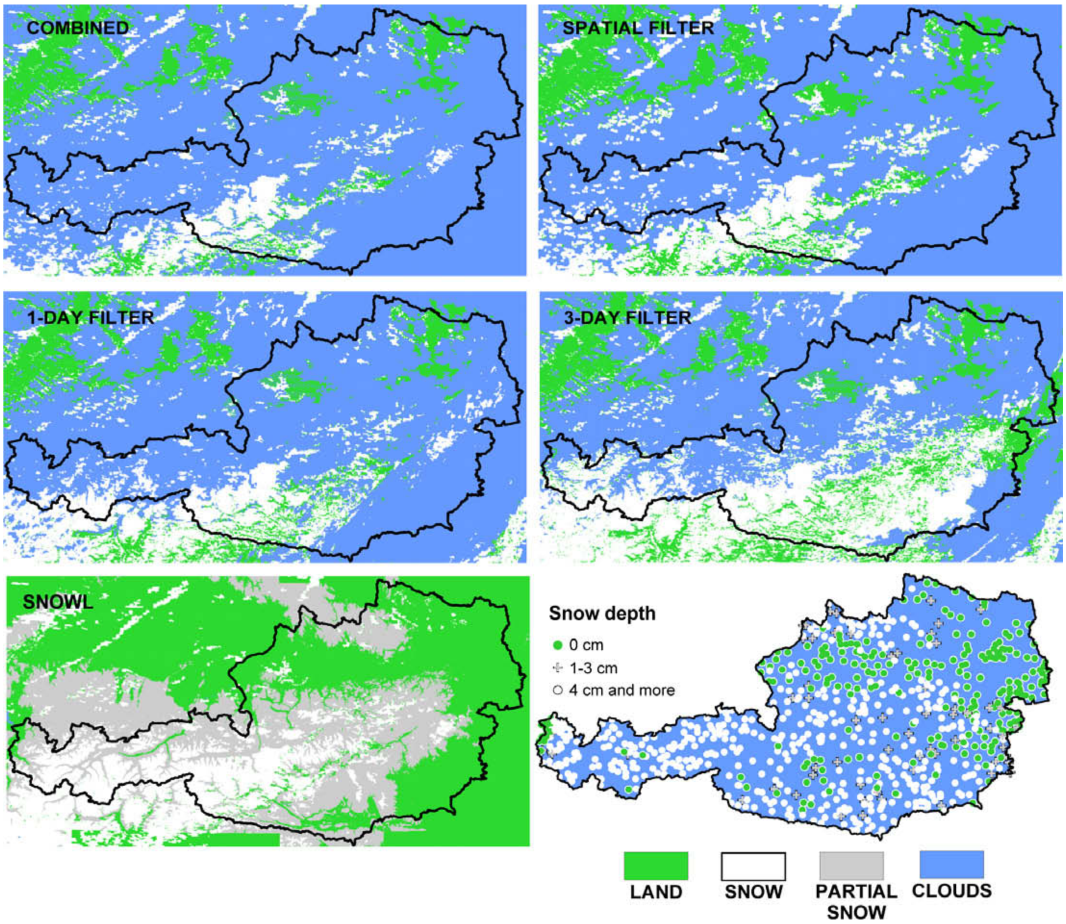

Fig. 10. Comparison of the *SNOWL* mapping method with spatial and temporal filters presented in Parajka and Blöschl (2008). Example for the same day as presented in Figs. 3 and 4 (January 23, 2003).

combined product, compared to 34% of the MODIS daily product. The increase in accuracy is somewhat smaller than that of Gao et al. (submitted for publication), who found an increase in the overall accuracy from 46.8% (MODIS/Terra) to 52.2% and 90.2% for the combined Terra–Aqua and the combination of Terra–Aqua with the passive AMSR-E datasets, respectively. However this analysis was performed in Alaska. The topography and snow regime in Alaska and Austria are different, so the mapping accuracies are not strictly comparable.

A regionally consistent evaluation is the comparison of the *SNOWL* method with the Terra–Aqua combination and spatial and temporal filters of Parajka and Blöschl (2008). Both studies are based on the same datasets, which enables us to draw more generic conclusions about the *SNOWL* mapping efficiency. The comparison indicates that the *SNOWL* provides a robust alternative especially to the temporal filters, which have similar potential for cloud reduction. A more favourable mapping performance of the *SNOWL* approach is found especially for cases when the snow covers starts to build or melt, which is documented by higher mapping accuracies in November, December and April. A typical example of such case is presented in Fig. 10, where snow cover depletion started in the flat, north-eastern, part of Austria. In this region, the *SNOWL* maps the snow cover remarkably closer to the snow depth observations than the temporal filters. A comparison of annual accuracies for cloud-free conditions and cloud coverage obtained for different mapping approaches is summarized in Table 3. The evaluation of the trade-off between accuracy and cloud reduction indicates that the 3-day filter of Parajka and Blöschl (2008) performs very similar to *SNOWL* with 98% cloud threshold. Interestingly, the *SNOWL* with 90% cloud threshold reduces somewhat more clouds than the 1-day filter and performs even slightly better than the original Terra/MODIS dataset. For Austria, the *SNOWL* method with 90% cloud threshold seems to be a reasonable choice for snow cover mapping.

The general benefits of the proposed mapping approach are the remarkable efficiency in cloud reduction and a good agreement with ground snow observations. The main strength is its simplicity and robustness. This concept was tested over Austria and can be easily adopted to regions with a similar vertical distribution of snow coverage. Apart from identifying snow cover per se, the method is useful for assisting in snow modeling (see, e.g., Blöschl and Kirnbauer, 1991, 1992). In the next studies we plan to test the *SNOWL* approach with the combined Terra–Aqua datasets and to evaluate the mapping performance for different spatial windows used for snow-line determination. Additionally we plan to refine the snow-line estimation accounting for different terrain aspects and topographic shading.

Acknowledgments

The authors would like to thank the Austrian Science Foundation (FWF Project No. P18993-N10) and the European Commission (AWARE Project, Contract No. SST 4-CT-2004-012257) for financial support and the Austrian Hydrographic Service (HZB) for providing the hydrologic data.

References

Blöschl, G., Kirnbauer, R., 1991. Point snowmelt models with different degrees of complexity – internal processes. Journal of Hydrology 129, 127–147.

Blöschl, G., Kirnbauer, R., 1992. An analysis of snow cover patterns in a small Alpine catchment. Hydrological Processes 6, 99–109.

Gao, Y., Xie, H., Lu, N., Liang, T., Xue, Ch., submitted for publication. Towards advanced daily cloud-free snow cover and snow water equivalent from Terra–Aqua MODIS and Aqua AMSR-E measurements. Journal of Hydrology.

Hall, D.K., Riggs, G.A., 2007. Accuracy assessment of the MODIS snow-cover products. Hydrological Processes 21, 1534–1547.

Hall, D.K., Riggs, G.A., Salomonson, V.V., Barton, J.S., Casey, K., Chien, J.Y.L., DiGirolamo, N.E., Klein, A.G., Powell, H.W., Tait, A.B., 2001. Algorithm theoretical basis document (ATBD) for the MODIS snow and sea ice-mapping algorithms. <http://www.modis-snow-ice.gsfc.nasa.gov/atbd01.html>.

Klein, A.G., Barnett, A.C., 2003. Validation of daily MODIS snow cover maps of the Upper Rio Grande River Basin for the 2000–2001 snow year. Remote Sensing of Environment 86, 162–176.

Liang, T., Zhang, X., Xie, H., Wu, C., Feng, Q., Huang, X., Chen, Q., 2008. Toward improved daily snow cover mapping with advanced combination of MODIS and AMSR-E measurements. Remote Sensing of Environment 112, 3750–3761. doi:10.1016/j.rse.2008.05.010.

Maurer, E.P., Rhoads, J.D., Dubayah, R.O., Lettenmaier, D.P., 2003. Evaluation of the snow-covered area data product from MODIS. Hydrological Processes 17, 59–71.

MODIS Reprojection Tool (MRT), 2004. Users Guide. Release 3.2a. Department of Mathematics and Computer Science, South Dakota School of Mines and Technology, USGS EROS Data Center, 58pp.

Parajka, J., Blöschl, G., 2006. Validation of MODIS snow cover images over Austria. Hydrology and Earth System Sciences 10, 679–689.

Parajka, J., Blöschl, G., 2008. Spatio-temporal combination of MODIS images – potential for snow cover mapping. Water Resources Research 44, W03406. doi:10.1029/2007WR006204.

Pepe, M., Brivio, P.A., Rampini, A., RotaNodari, F., Boschetti, M., 2005. Snow cover monitoring in Alpine regions using ENVISAT optical data. International Journal of Remote Sensing 26 (21), 4661–4667.

Pu, Z., Xu, L., Salomonson, V., 2007. MODIS/Terra observed seasonal variations of snow cover over the Tibetan Plateau. Geophysical Research Letters 34, L06706. doi:10.1029/2007GL029262. 6p.

Riggs, G.A., Hall, D.K., Salomonson, V.V., 2003. MODIS snow products user guide for collection 4 data products. <http://modis-snow-ice.gsfc.nasa.gov/sug_main.html>.

Seidel, K., Lichtenegger, J., Ade, F., 1983. Augmenting LANDSAT MSS data with topographic information for enhanced registration and classification. IEEE Transaction on Geoscience and Remote Sensing 21, 252–258.

Seidel, K., Ehrler, C., Martinec, J., 1996. Multisensor analysis of satellite images for regional snow distribution. In: Parlow, E. (Ed.), Progress in Environmental Research and Applications, 15th EARSeL Symposium 1995, Basel, Switzerland, A.A. Balkema, Rotterdam/Brookfield, pp. 213–220.

Simic, A., Fernandes, R., Brown, R., Romanov, P., Park, W., 2004. Validation of VEGETATION, MODIS, and GOES + SSM/I snow cover products over Canada based on surface snow depth observations. Hydrological Processes 18, 1089–1104.

Tong, J., Dery, S.J., Jackson, P.L., 2009. Interrelationships between MODIS/Terra remotely sensed snow cover and the hydrometeorology of the Quesnel River Basin, British Columbia, Canada. Hydrology and Earth System Sciences 13, 1439–1452.

Wang, X., Xie, H., Liang, T., Huang, X., 2008. Comparison and validation of MODIS standard and new combination of Terra and Aqua snow cover products in northern Xinjiang, China. Hydrological Processes. doi:10.1002/hyp.7151.

Xie, H., Wang, X., Liang, T., 2009. Development and assessment of combined Terra and Aqua snow cover products in Colorado Plateau, USA and northern Xinjiang, China. Journal of Applied Remote Sensing 3, 033559. doi:10.1117/1.3265996.

Zhou, X., Xie, H., Hendrickx, J.M.H., 2005. Statistical evaluation of remotely sensed snow cover products with constraints from streamflow and SNOTEL measurements. Remote Sensing of Environment 94, 214–231.